

We are IntechOpen, the world's leading publisher of Open Access books Built by scientists, for scientists

4,800

Open access books available

122,000

International authors and editors

135M

Downloads

Our authors are among the

154

Countries delivered to

TOP 1%

most cited scientists

12.2%

Contributors from top 500 universities



WEB OF SCIENCE™

Selection of our books indexed in the Book Citation Index
in Web of Science™ Core Collection (BKCI)

Interested in publishing with us?
Contact book.department@intechopen.com

Numbers displayed above are based on latest data collected.
For more information visit www.intechopen.com



Evaluating the Progress of Atmospheric Research in Understanding the Mechanics Behind Tropical Cyclone-Induced Tornadogenesis

Jordan L. Rabinowitz

Additional information is available at the end of the chapter

<http://dx.doi.org/10.5772/64142>

Abstract

As tropical cyclones make landfall along coastlines all over the world, havoc is wreaked on families, businesses, economies, etc. A generally overlooked topic is one of the inherent dangers in tropical cyclone landfalls. These can produce tornadoes in the spiral rain bands coming ashore by encountering increasingly higher frictional convergence. The second component will be assessing which other parameters could be analyzed on a synoptic timescale to evaluate how we can potentially improve longer term predictions of tropical cyclone (TC)-induced tornadogenesis. The analysis showed that the combination of high low-level moisture, vertical temperature gradients, and enhanced vertical wind shear is the key factor that links landfalling tropical cyclones to associated tornadogenesis prior to, during, and/or after the time of landfall. An integral part of the process preceding TC-induced tornadogenesis is the enhanced vertical temperature gradient that develops as the storm maintains warm-core characteristics aloft but develops cold-core characteristics closer to the surface. The examination of forecaster perspectives showed that over the past few years there is strong evidence of forecaster improvement based upon greater cognizance of forecast variables linked to TC-induced tornadoes.

Keywords: tropical cyclones, landfall, tornadoes, frictional convergence, energy helicity index, low-/mid-level lapse rates

1. Introduction

Amidst the added pressures associated with forecasting landfalling tropical cyclones (TCs), tornadic supercells embedded in the outer spiral rain bands are of particular concern to

operational forecasters. As the United States has become more industrialized, a larger percentage of the population has settled in coastal regions. As a consequence, the inherent dangers linked to landfalling TCs have become a more prevalent issue as more people are living in areas which are geographically and economically vulnerable to TCs [1, 2]. TC-induced tornadoes can occur during the evening or overnight hours, complicating visual confirmation due to the lack of daylight and/or being rain-wrapped. One of the goals associated with TC forecasting is the accurate anticipation of the timing and location of tornadogenesis with respect to a TC landfall. The tornadoes that do occur in association with TCs are rated based upon the Enhanced Fujita (EF) damage rating scale. A large portion of TC-induced tornadoes are of EF-2 intensity or weaker (maximum winds up to 117 kts), with a small percentage reaching EF-3 (maximum winds between 118 and 143 kts) and even more rarely EF-4 intensity (maximum winds between 144 and 174 kts) [3, 4]. This is reflected in **Figure 1** that illustrates the TC-tornado intensity breakdown based on the analysis in Tropical Cyclone Tornado Records for the Modernized NWS Era [4].

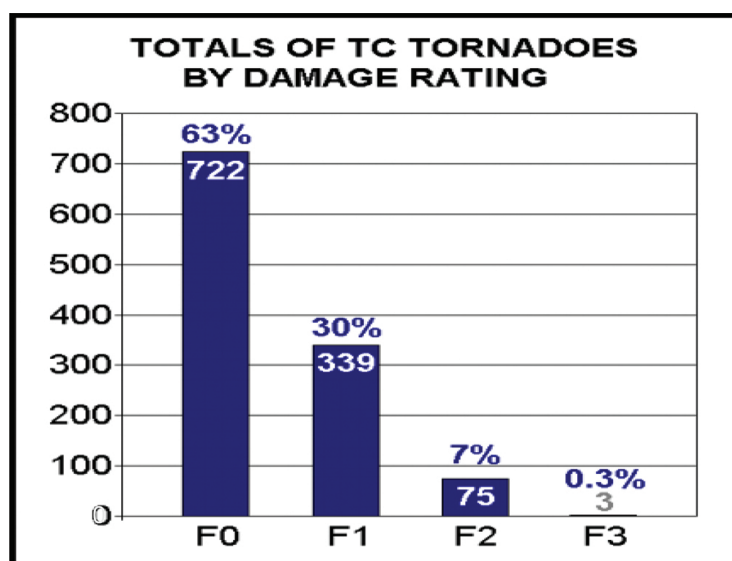


Figure 1. The breakdown of the percentage and number of the 1139 tornadoes that occurred between 1995 and 2009 TC based on their damage rating [4].

The motivation for presenting the content in this chapter is twofold. The first part involves revisiting previous research and assessing how it has benefited the atmospheric research and forecasting communities over the past few decades. The second part is assessing where atmospheric research needs to head moving forward based on the forthcoming results being presented. This chapter is organized as follows. Section 2 consists of an inclusive literature review covering 47 years of TC-induced tornadogenesis research, focusing on relevant statistics and dynamics. Section 3 presents an overview of the data sources that were utilized and the methods by which different contents were evaluated. Section 4 provides a detailed explanation of the results that are divided into two parts: a comprehensive synoptic analysis of 44 United States TC landfall events and detailed analyses of operational forecaster perspectives from the Storm Prediction Center (SPC). The objective of the SPC is to “deliver timely

and accurate watch and forecast products/information dealing with severe weather, wildfires, and winter weather for the United States to protect lives and property” (<http://www.spc.noaa.gov>).

2. Literature review

Past research involving TC-induced tornadogenesis dates back to the middle of the twentieth century. The onset of the satellite era stimulated the atmospheric research community to study mesoscale features embedded within synoptic-scale systems more comprehensively. A paramount issue is the forecasting of tornadoes induced by landfalling TCs along the United States mainland. Over the past six decades considerable progress has been made in understanding the atmospheric dynamics associated with TC-induced tornadogenesis. Early work, which studied TC-induced tornadogenesis, primarily focused on the collection of tornado reports and generating initial theories to explain the variable occurrence of tornadoes during TC landfall events [5, 6].

The work of Smith [6] was composed of compiling a TC-induced tornado climatology using tornado reports from 1955 to 1962. This work proposed a climatological TC tornadogenesis model based on the forward speed of TCs as well as influences from the dynamically driven frictional convergence and strong low-level vertical shear in the northeast quadrant of landfalling TCs. It was noted that some tornado reports are marginal due to the issues such as insufficiently educated spotter reports and/or limited remote sensing capabilities. Nonetheless, this earlier work provided the basis for further progress, starting with Pearson and Sadowski's work [5]. Their work expanded upon [6] by conducting a more detailed assessment of location and timing of tornadogenesis relative to the TC center position. The work of Pearson and Sadowski [5] also provided evidence for tornadogenesis occurring 12 h or more ahead of the arrival of hurricane-force winds. This discovery was monumental as it showed that TC-induced tornadoes occur farther from the center than previously believed.

Novlan and Gray [7] analyzed TC-induced tornadogenesis reports between 1948 and 1972 for the United States and between 1950 and 1971 for typhoons that impacted Japan. The compiled analysis of tornado reports revealed that the number of tornadoes initiated by a given TC was regulated by the rate of cooling aloft, the change in wind speed from the surface to 850 mb, and rising surface pressure values near the TC center upon landfall. It was found that tornadic TCs had weaker winds at the surface and stronger winds aloft, or stronger vertical wind shear [7–9]. In addition, the ambient surface temperatures of tornadic TC environments were lower than those which did not produce tornadoes. The temperatures at 850 mb also remained high in both scenarios, indicating the presence of a low-level cold core that maintained a stronger vertical wind shear profile [7]. This process enhanced cumulus downdraft potential, supporting stronger low-level horizontal wind shear based on a stronger vertical temperature gradient within the tornadic TC environments. Consequently, this induced intense small-scale regions of convergence and rotation, which were objectively associated with the TC-induced tornadogenesis [7].

Moving into the 1980s, Gentry [8] studied TC-induced tornado reports between 1973 and 1980 coupled with considerations based on past research. A core part of his work was appending data from [7] to develop a more comprehensive analysis of tornado reports based on their position relative to the coastline and their distance from TC center positions. A major finding was the majority of tornadoes occurred within 100 km of a given TC center and/or between azimuths of 20° and 120° . The results from [8] reaffirmed that strong vertical wind shear and strong vertical temperature gradients (i.e., cold-core to warm-core changes with height in tornadic TCs) are most responsible for generating environments conducive for tornadogenesis.

In the 1990s, McCaul and Weisman [10] studied composite profiles of temperature, moisture, and wind fields coincident with tornadic TC environments between 1948 and 1986. The premier finding was that helicity (i.e., helical flow) and vertical wind shear parameters were best correlated with TC-induced tornadogenesis. A second major finding was that the number and intensity of TC-induced tornadoes increased in accordance with the increasing TC size and intensity. A final important result from this work was that TCs landfalling along the East Coast produced fewer tornadoes than those that made landfall along the Gulf Coast. Spratt et al. [11] analyzed tornadic mesocyclones associated with two mature TCs that were not close to landfall near the time of tornadogenesis (i.e., Tropical Storm Gordon (1994) and Hurricane Allison (1995)). The primary result was the confirmation of several similarities between TC-induced tornadic cells and Great Plains supercells. In spite of the TC-induced convection being much lower-topped, the ratio of the depth of rotation to storm top was comparable between TC-induced tornadic cells and more common Great Plains supercells. The shallower depth of these rotating cells presented the issue of nondetection based on weaker capabilities of the Weather Surveillance Radar-1988 Doppler (WSR-88D) radar technology. Another important similarity was the persistent nature observed within both Great Plains supercells and TC-induced tornadic supercells.

Heading into the twenty-first century, many breakthroughs advanced the comprehension of dynamics relevant to TC-induced tornadogenesis. The focus of McCaul et al. [12] was studying the remnants of Tropical Storm Beryl (1994) with data from the WSR-88D radar at Columbia, South Carolina, and the National Lightning Detection Network. A major finding was the persistence of offshore low-topped supercells, one of which lasted 11 h and generated multiple tornadoes based on radar data over the course of 6.5 h. In addition, many cases showed a decrease in the frequency of cloud-to-ground (CG) lightning strikes or no lightning activity at all within 30 min of tornadogenesis [12]. Schultz and Cecil [3] conducted a detailed analysis of 1800 TC-induced tornadoes that occurred between 1950 and 2007 to develop an even more extensive TC-tornado climatology as shown in **Figure 2**. Their results supported hypotheses from previous work regarding the differences between inner- and outer-region tornadoes within TC circulations [6, 7]. Another major finding was that the outer-region tornadoes (greater than 200 km from the TC center) exhibited a stronger diurnal signal, with many tornadoes occurring in the afternoon. On the other hand, inner-region tornadoes typically occurred within about 12 h of landfall (without preference for time of day). As stated in [8], the majority of TC tornadoes (60%) occurred within 100 km of the coast. These events include all of the tornadoes in close proximity to the TC core near the time of landfall as well as

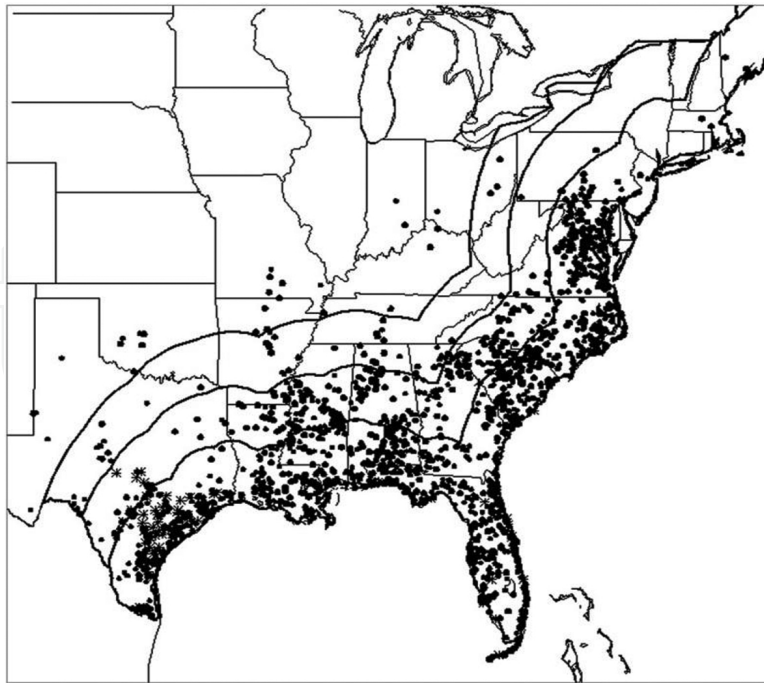


Figure 2. The 1800 tornadoes plotted within the ranges of 200, 400, and 600 km from the respective United States coastlines [3].

tornadoes embedded in rain bands far from the TC center. The last major finding was that the tornadic threat can be found to persist for 2–3 days after landfall and as far as 400–500 km inland from the TC center [3, 13].

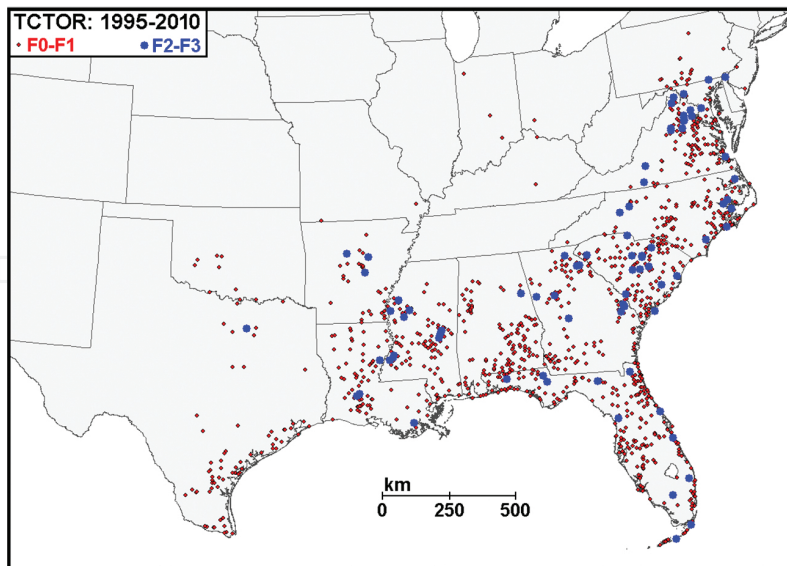


Figure 3. A map of initiation points of 1163 United States TC-induced tornadoes which occurred between 1995 and 2010, damage rating 48 bins as labeled [4].

Edwards [14] studied a TC-tornado dataset dating from 1995 to 2009 from which various graphical and statistical analyses were generated. He conducted a detailed analysis of the position and intensity of 1139 tornadoes that occurred in association with TCs during this 15-year period as shown in **Figure 3**. One revealing result was that the 1139 tornadoes broke down such that there were 722 F0-tornadoes (63.39%), 339 F1-tornadoes (29.76%), 75 F2-tornadoes (6.58%), and 3 F3-tornadoes (0.26%). This statistical breakdown revealed that an overwhelming percentage of the TC-induced tornadoes were characterized by a weaker intensity (i.e., winds of 63 kts or less). The aforementioned TC-induced tornado distribution is comparable to tornado statistics from 1970 to 2002, which were compiled by McCarthy and Schaefer [15]. Within the aforementioned 32-year tornado climatology, the following intensity percentage distribution was found: 39, 36, 19, 5, and 1% for F0, F1, F2, F3, and F4 tornadoes, respectively [15]. The second finding was the apparent peak hours of TC-induced tornado occurrence between 18:00 UTC and 00:00 UTC as reflected in **Figure 4** [14]. This 6-h window in which TC-induced tornadoes occurred most frequently provided evidence for the strong influence of the diurnal cycle on these times of tornadogenesis. This highlighted the importance of diabatic heating and its influence on convective available potential energy (CAPE) values.

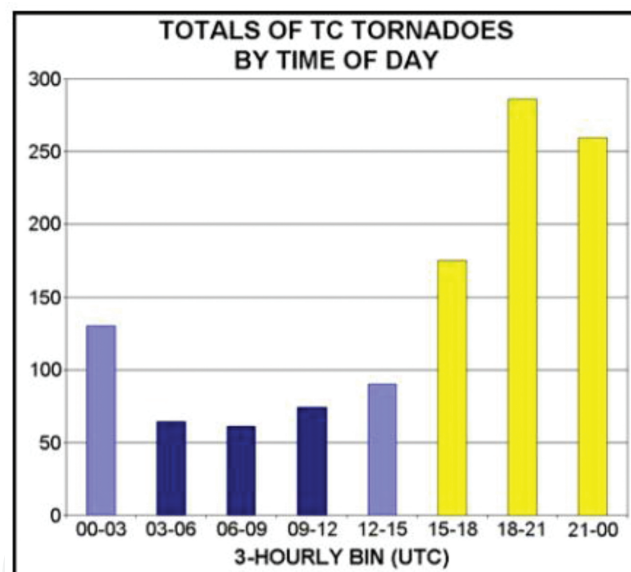


Figure 4. TC-tornado events by UTC time, in 3-hourly groupings. Yellow bars correspond to the local diurnal cycle 19 along the Gulf and Atlantic Coasts, while dark blue bars correspond to the nocturnal cycle. Purple bars correspond to the period of transition between the maximum diurnal cycle impacts and the overnight hours. Periods end in the minute 20 before the labeled times, e.g., “21–00” covers 2100–2359 UTC [4].

Edwards et al. [16] studied a 2003–2011 subset of the Storm Prediction Center (SPC) TC tornado records dataset in conjunction with environmental convective parameters derived from the SPC’s hourly mesoscale analysis archive. A key difference observed between TC and non-TC tornado environments was that TC-tornado environments exhibited deeper tropospheric moisture coupled with the reduced lapse rates (near moist adiabatic) and lower CAPE. There was also a proposed objective, which is to study TC-tornado environments more consistently

in order to provide higher-quality data in real time, which may improve the overall effectiveness of operational forecasts in TC-tornado prone locations.

3. Data and methods

A core element of this chapter was analyzing 44 potential TC-tornado events between 2001 and 2015 across the Tropical Atlantic basin. An event was designated as any 24-h period in which a TC was near (within ~160 km) or making landfall along the United States Gulf Coast or East Coast. The critical part of the data collection involved differentiating TC tornadoes vs. tornadoes associated with other mesoscale and/or synoptic-scale systems. This was accomplished by comparing the location and track of a given TC with the positions of reported tornadoes. The final step was analyzing the evolution of available radar data to confirm or reject the validity of reported tornadoes based on the timing of the reports with respect to TC progression.

The first major component of this work was conducting comprehensive synoptic analyses of the lower, middle, and upper levels (as well as an array of model-derived products). These synoptic analyses focused on specified mandatory levels (i.e., 300, 500, 700, 850 mb, and the surface) in conjunction with several model-derived products (see below) from the SPC's hourly mesoscale analysis archive. It is important to note that these model-derived products became fully available from 18 October 2005. Between 3 May 2005 and 17 October 2005, data were only available from 17:00 UTC to 03:00 UTC on the following day (11 out of 24 h per event), limiting the number of consecutive hours available for assessment during that 5-month timeframe.

The model-derived products being analyzed include 0–1-km energy helicity index (EHI), 0–3-km EHI, 100 mb mean parcel lifted condensation level (LCL) height (meters AGL), 300 mb height/divergence/wind, 500 mb height and vorticity, 500, 700, and 850 mb heights/temperatures/winds (measured in decameters, degrees Celsius, and knots), 850 mb moisture transport vector (measured as the product of the wind speed (m/s) and the mixing ratio (g/g) at 850 mb), 850 mb temperature advection (measured as the increasing or decreasing temperature trend) (i.e., positive values indicative of warm-air advection vs. negative values indicative of cold-air advection), Bulk Richardson Number (BRN) shear (m^2/s^2), effective bulk shear (kts), mean sea-level (MSL) pressure, and precipitable water (inches). Among the 44 events, only 26 events have near/fully complete data sets (June 2005 through June 2015). In addition, some data were missing for 12 events between June 2005 and June 2007, limiting data analysis somewhat during that timeframe.

4. Results

4.1. Environmental analysis

A major facet of this work was conducting in-depth synoptic analyses of 44 individual events that occurred between 2001 and 2015. The first part of this analysis focused on the evolution

of the upper-level dynamics by looking at 300 mb heights, divergence, and winds. The main focus was assessing upper-level divergence with respect to the number of tornadoes that occurred during each event. The average maximum value for 300 mb divergence among the 44 events was $4.32 \times 10^{-5} \text{ s}^{-1}$, whereas the majority of tornadic TCs had divergence values between 4 and $6 \times 10^{-5} \text{ s}^{-1}$ (see **Table 1**). This suggests that upper-level divergence had at least some influence on tropospheric mass evacuation near convective cells moving ashore by enabling thunderstorm updrafts to reach higher altitudes. However, previous work has established that low- and mid-level dynamics play a larger role in TC-induced tornadogenesis [5, 7, 8, 17].

In examining the middle levels, the analyzed parameters included 500 mb heights/temperatures/winds and 500 mb height and absolute vorticity. Collectively, the 500 mb height, temperature, and wind values had respective average values of 580.35 dm, -4.33°C , and 35.47 kts. For the most tornadic TCs, the majority of 500 mb height values ranged between 5 dm above and below the average value. The 500 mb temperature values had a larger range of variability, with the most tornadic TCs having values range from -8 to 5°C . For the most tornadic TCs, the 500 mb wind values ranged from 25 to 60 kts. The second aspect evaluated at the 500 mb level was 500 mb height and absolute vorticity (for the 15 data-ready cases) for which the average value was $37.47 \times 10^{-5} \text{ s}^{-1}$. It is important to note that the 500 mb vorticity values ranged from 24×10^{-5} to $58 \times 10^{-5} \text{ s}^{-1}$, indicating that greater vorticity was not correlated with increasingly tornadic TCs. For a deeper look into these mid-level parameters, refer **Table 1** for average value comparisons between all of the events and the most tornadic events.

In stepping down to lower levels, 700 mb heights, temperatures, and winds were the focus. For the most tornadic TCs, the average 700 mb height value was calculated to be 306.16 decameters. Yet, among the various case studies, the 700 mb height values range from 292 to 316 dm. This indicated that the most tornadic TCs occurred with both below- and above-average 700 mb heights, suggesting that the proximity of the TC center to the coastline may have played a key role. As a landfalling TC moves inland, the associated pressure gradient weakens and the lowest minimum central pressure rises. This process is a direct consequence of the transient balance between the rate of mass adjustment toward the center (i.e., via cyclonic inflow toward the TC center) and the rate of tropospheric mass evacuation [3, 7]. The most tornadic TCs, occurring with above-average heights, likely unfolded due to rising mid-level heights coupled with a conditionally unstable convective boundary layer during the post-landfall phase of a particular TC [3, 9, 11]. In examining the 700 mb temperatures, the average value was 9.34°C , and most tornadic TCs were close to this value when measured near the height of each event. By analyzing the 700 mb winds, the average value came out to be 39.09 kts. However, during the most tornadic TCs, the 700 mb wind values ranged from 25 to 90 kts, which is higher than the typical values. For these lower level parameters, refer **Table 1** for comparisons of the average values for all of the events as compared to the most tornadic events. During some landfalling TCs in which 30 or more tornadoes were reported, the mean effective bulk shear value was 40 kts; thus, it is plausible that the larger number of tornadoes was due to larger magnitudes of the low-level shear, coupled with the 850 mb wind data and other low-level data discussed below.

Critical TC-induced tornado parameter averages						
Parameter (number of data- ready cases)	300 mb divergence (10^{-5} s^{-1}) (44 cases)	500 mb height (dam) (44 cases)	500 mb temperature ($^{\circ}\text{C}$) (44 cases)	500 mb wind speed (kts) (44 cases)	500 mb absolute vorticity (10^{-5} s^{-1}) (15 cases)	
Total event average	4.32	580.35	-4.33	35.47	37.47	
Most tornadic event average (10 + tornadoes)	4.67	578.57	-3.57	41.43	39.14	
Parameter (number of data- ready cases)	700 mb height (dam) (44 cases)	700 mb temperature ($^{\circ}\text{C}$) (44 cases)	700 mb wind speed (kts) (44 cases)	850 mb height (dam) (44 cases)	850 mb temperature ($^{\circ}\text{C}$) (44 cases)	850 mb wind speed (kts) (44 cases)
Total event average	306.16	9.34	39.1	142.41	17.14	40.91
Most tornadic event average (10 + tornadoes)	303.95	9.57	44.76	139.81	16.9	46.48
Parameter (number of data- ready cases)	0–1 km EHI (26 cases)	0–3 km EHI (26 cases)	100 mb mean parcel LCL height (m AGL) (26 cases)	BRN shear (kts) (26 cases)	Effective bulk shear (kts) (26 cases)	Mean sea- level pressure (mb) (44 cases)
Total event average	2.83	3.31	640.38	106.4	41.74	985.55
Most tornadic event average (10 + tornadoes)	2.75	3.29	625	130	44.17	982

Table 1. Total events average and most tornadic event average values for 300 mb divergence, 500 mb heights/temperatures/winds and absolute vorticity, 700 mb heights/temperatures/winds, 850 mb heights/temperatures/winds, 0–1 and 0–3 km EHI, 100 mb mean parcel LCL height, BRN shear, effective bulk shear, and mean sea-level pressure.

Further, low-level analysis involved examining the 850 mb heights/temperatures/winds, 850 mb moisture transport vector, and 850 mb temperature advection (the last two parameters only having 15 data-ready cases). The average 850 mb height, temperature, and wind values were calculated to be 142.41 dm, 17.14 $^{\circ}\text{C}$, and 40.91 kts. A critical finding was that the 850 mb heights associated with the more tornadic TCs were near or below the average value, indicating that lower 850 mb heights favored more tornadoes, which agreed with the previous work [7]. For the most tornadic TCs, 850 mb temperatures stayed near or below average, illustrating that TCs which maintained lower mid-level temperatures tended to produce more tornadoes. This is a result of those TCs maintaining warmer near-surface temperatures and cooler mid-level temperatures, strengthening vertical wind shear, which is a critical aspect of TC-induced tornadogenesis. This concurs with the previous work finding that TCs that maintain a warm-core structure aloft, while developing a cold-core structure near the surface, develop stronger vertical wind shear [7]. Consequently, this stronger vertical wind shear fosters an environment

more conducive for TC-induced tornadogenesis. Finally, 850 mb wind speeds for the larger tornado producing TCs were at or above the average value, indicating that stronger low-level winds are more favorable for tornadogenesis assuming the presence of weaker winds at the surface. For the 850 mb parameters, refer **Table 1** for comparisons of the average values for all of the events as compared to the most tornadic events.

Another important component was the 850 mb moisture transport (flux) vector, which is the product of the wind speed (m/s) and the mixing ratio (g/g) at 850 mb. This product (studied for 15 data-ready cases) showed that within 12 h of TC-tornadogenesis, there was a large quantity of warm/moist air advected into the tornadic regions. This provided abundant water vapor, which has been shown to be crucial for TC tornadogenesis as well as more common Great Plains tornadic supercells [9, 18]. The last 850 mb product being analyzed was 850 mb temperature advection that among the 15 data-ready events had an average value of $-2.31 \times 10^{-5} \text{C s}^{-1}$. It was found that 850 mb temperature advection among the most tornadic TCs ranged from 10×10^{-5} to $-20 \times 10^{-5} \text{C s}^{-1}$ near the time of maximum tornadogenesis. More specifically, this meant that during the most tornadic TCs there was either weak warm-air advection or weak/moderate cold-air advection occurring on a 3 h timescale. Taking past research into consideration, it makes sense that the most tornadic TCs occurred with below-average 850 mb temperatures [7]. For cases with lower 850 mb temperatures, more research is needed to better understand why comparable numbers of tornadoes occur when the vertical temperature gradient is weaker.

Other critical components of TC-induced tornadogenesis include the presence of vertical wind shear and more near-surface variables. In regards to the near-surface domain, analyses were conducted for 0–1 km EHI, 0–3 km EHI, 100 mb mean parcel LCL height (measured in meters AGL), BRN shear, effective bulk shear, MSL pressure, and precipitable water depth (all of which had only 26 data-ready cases except for MSL for which data were available for all 44 events). Taking the EHI into consideration, it is worth noting that the representative equation is

$$\text{EHI} = \left(\frac{\text{CAPE}}{\text{storm} - \text{relative helicity}} \right) \times 160,000;$$

which is the ratio between CAPE and low/mid-level wind shear represented by storm-relative helicity, which indicates the relative importance of each variable. The average values for 0–1 km EHI and 0–3 km EHI were 2.83 and 3.31, respectively, with the most tornadic TCs having greater than average values for both variables. This indicates the greater value of buoyancy relative to wind shear for tornado producing events. In addition, EHI values larger than one indicate a greater potential for tornadoes up to EF-3 strength, this is a very propitious result that needs to be further evaluated as also discussed by Eastin and Link [19]. The next parameter evaluated was the 100 mb mean parcel LCL height that was given in meters AGL. The average value for the 100 mb mean parcel LCL heights was calculated to be 640.38 m AGL for the 26 data-ready cases. Most tornadic TCs had 100 mb mean parcel LCL heights ranging from 140

m AGL below to 100 m AGL above average. This provided supporting evidence that lower LCL heights are more favorable for TC-induced tornadogenesis (i.e., 100 mb mean parcel LCL heights under 1000 m AGL) [9, 19]. For these near-surface parameters, refer to **Table 1** for comparisons of the average values for all of the events as compared to the most tornadic events.

The last part of the synoptic analysis considered the following variables: BRN shear, effective bulk shear, MSL pressure, and precipitable water depth. BRN shear is the square of the bulk vector difference between the 0 and 500 m AGL mean wind (both pressure weighted) and then multiplied by one half (<http://www.spc.noaa.gov>). It has been found that higher BRN values are linked to an increasing risk of supercells based on BRN values being defined by the ratio of buoyancy and shear. This supports the findings from the EHI analyses, which is contingent upon the ratio of convective available potential energy (CAPE) and wind shear in the form of storm-relative helicity [11]. The average BRN shear value was $106.4 \text{ m}^2 \text{ s}^2$, whereas the most tornadic TCs had values ranging between 80 and $220 \text{ m}^2 \text{ s}^2$. This is important because BRN shear values at or above $40 \text{ m}^2 \text{ s}^2$ support environments more conducive for TC-induced tornadogenesis [20]. Looking at effective bulk shear, the average value was calculated to be 41.74 kts, whereas the most tornadic TCs had values ranging from 40 to 60 kts. This is important based on previous work finding that supercell development becomes more likely as effective bulk shear increases to 25–40 kts or greater (<http://www.spc.noaa.gov>). Upon inspecting the evolution of precipitable water, it became clear that values in the vicinity of a landfalling TC were consistently over 2.00 in. This concurs with previous work finding that high water vapor content is essential for TC-induced tornadogenesis due to the necessity for deep moisture within the convective boundary layer [8, 9, 16, 19]. For these additional near-surface parameters, refer to **Table 1** for aforementioned average value comparisons.

The final aspect being assessed is mean sea-level pressure, whose average value among the 44 events was calculated to be 985.55 mb. It is important to mention that the lowest mean sea-level pressure values were all calculated when the storm was approaching landfall (i.e., the TC center was within 160 km of the coastline). For the most tornadic TCs, the mean sea-level pressure values ranged anywhere from 949 to 1008 mb. This indicated significant variability among the surface pressures of landfalling TCs, suggesting that a more intense TC at the time of landfall does not directly correlate with the production of more tornadoes. However, previous work has shown that the majority of tornadoes occur with rapidly weakening TCs upon landfall (i.e., TC centers rapidly filling in terms of the net mass adjustment) [7]. For a more detailed comparison of the average values for all of the events as compared to the more tornadic events, refer to **Table 1**.

4.2. Forecast analysis

By examining this issue with a social impact perspective, it is clear that the public's information outlet is contingent upon the communication of operational meteorologists. This section is a detailed analysis of 124 archived mesoscale discussions from the SPC beginning in August 2004. The forecasters responsible for these mesoscale discussions include the following: C. Broyles, G. Carbin, Dr. A. Cohen, S. Corfidi, M. Darrow, S. Dial, R. Edwards, S. Goss, J. Grams, J. Hart, R. Jewell, B. Kerr, E. Leitman, Dr. P. Marsh, M. Mosier, J. Peters, J. Picca, J. Rogers, R.

Thompson, B. Smith, and the late Jonathan Racy. The impetus for studying these archived mesoscale discussions was to look for a trend in forecaster improvement over the last 10–15 years. The primary focus was assessing the timeliness and accuracy of warnings conveyed by forecasters. Mesoscale discussions for events during and after 2004 were chosen since that was when the SPC began publishing graphics to visually illustrate their dialogue. The addition of graphics provided further insight into the thoughts of forecasters during a particular situation. The principal factors being studied were the number of times the following words appeared at least once in a given discussion: high temperature(s) or surface heating, instability (i.e., CAPE (the amount of energy available for convection), SBCAPE(surface-based CAPE → the value of CAPE relative to an air parcel rising from the lower planetary boundary layer), MLCAPE(mixed-layer CAPE → CAPE calculated with values of temperature and moisture from the lowest 100 mb above ground level), DCAPE(downdraft-CAPE → CAPE calculation which estimates the strength of rain and evaporatively cooled downdrafts), wind shear (i.e., bulk shear, low-level shear, sheared profile, etc.), storm relative helicity (SRH) in the 0–1 or 0–3 km layer, and precipitable water (<http://www.spc.noaa.gov>). The intention was to assess which factors were most critical for TC-induced tornadogenesis from the standpoint of SPC mesoscale forecasters.

Of the 124 mesoscale discussions, 49 discussions (39.52%) had at least one mention of surface heating and/or high temperatures. Then, 47 of the 124 discussions (37.90%) contained at least one mention of instability terminology. Also, 100 of the 124 discussions (80.65%) contained at least one mention of wind shear terminology. In addition, 66 of the 124 discussions (53.23%) contained at least one mention of storm relative helicity terminology. Finally, 7 of the 124 discussions (5.65%) contained at least one mention of precipitable water. Collectively, wind shear was a prominent topic of many discussions, coinciding with the past research findings that strong low-level wind shear is essential for TC-induced tornadogenesis [10, 16].

In addition, the frequent presence of surface heating and/or high temperature wordings, instability terminology, and storm-relative helicity terminology indicated the issues' prevalence to forecasters involved in watch and/or warning coordination [14]. The main point ascertained from the relative frequency of the discussion parameters from 2004 to 2015 is that SPC forecasters clearly have improved during the latter dual-polarization era that began in late mid to late 2012 across much the contiguous United States (particularly along the Gulf and East Coast regions). This margin of improvement is distinguished by a greater presence of wind shear terminology that as previously stated is crucial to TC-induced tornadogenesis. This may suggest that advanced remote sensing capabilities, as in the implementation of dual-polarization radar technology, in concert with high-resolution rapid-scan satellite imagery, have bolstered forecaster analysis quality.

5. Conclusions

Given the growth of the global population, especially those living near coastlines, and the consistent threats associated with landfalling TCs, there is a growing need for improvements

to the modeling and forecasting of TC intensities and trajectories. As a nearly 50-year period of research has shown, tremendous progress has been made in understanding the dynamics that govern TC-induced tornadogenesis. Yet, considerable work still awaits the atmospheric science community.

The results of the environmental analysis showed that upper- and mid-level factors help facilitate TC-induced tornadogenesis. In some cases, upper-level divergence appeared to support tropospheric mass evacuation, bolstering upward vertical velocities within convective cells. It is imperative to note that upper-level divergence was not essential based on several cases with 10+ tornadoes occurring without significant upper-level divergence. Inspecting the middle levels, 500 mb heights/temperatures/winds experienced notable variability that was likely due to differences prior to and after landfall (i.e., pre-landfall TCs were associated with lower 500 mb heights, lower 500 mb temperatures, and stronger 500 mb wind speeds, whereas post-landfall tornadic TCs were the opposite coupled with a greater tendency for synoptic interactions). In regards to 500 mb absolute vorticity, larger values were not synonymous with greater tornado production.

Analysis of 700 and 850 mb data revealed that most tornadic TCs occurred with at or below-average heights, near-average temperatures, and above-average winds. The tendency for at or below-average heights coupled by near-average temperatures (i.e., average values being 9.34°C at 700 mb and 17.14°C at 850 mb) backs the presence of a notable vertical temperature gradient that is pivotal in facilitating TC-induced tornadogenesis. Approaching the surface, the variables, i.e., 100 mb mean parcel LCL heights, BRN shear, effective bulk shear, and mean sea-level pressure, showed convincing output (as shown in **Table 1**). Collectively, it is clear that the essential components most responsible for TC-induced tornadogenesis reside within the planetary boundary layer coupled with some relevant mid-level factors.

However, as with many aspects of meteorology, no individual numerical weather prediction product (i.e., a deterministic model forecast) can be the sole product with which we determine the likelihood of a particular TC producing or not producing tornadoes. Rather, it is with the integration of ensemble forecasts and appropriate temporal and/or spatial parameterizations that atmospheric research will fortify additional headway in generating more accurate TC forecasts. By the collaborative efforts of both atmospheric researchers from the United States and other countries around the world, this is the method by which atmospheric science will most productively push forward in this pursuit of knowledge.

Author details

Jordan L. Rabinowitz

Address all correspondence to: jlrxw6@mail.missouri.edu

Department of Soil, Environmental, and Atmospheric Sciences, University of Missouri,
Columbia, MO, United States

References

- [1] Pielke, R A, Landsea C W. La Niña, El Niño, and Atlantic Hurricane Damages in the United States. *Bull. Am. Meteorol. Soc.* 1999; 80: 2029–2032. DOI: 10.1175/1520-0477(1999)080<2027%3ALNAENO>2.0.CO%3B2
- [2] Pielke, R A, Gratz J, Landsea C W, Collins D, Saunders M A, Musulin R. Normalized Hurricane Damage in the United States: 1900–2005. *Nat. Hazards Rev.* 2008; 31: 29–38. DOI: 10.1061/(ASCE)1527-6988(2008)9:1(29)
- [3] Schultz, L A, Cecil D J. Tropical Cyclone Tornadoes, 1950–2007. *Mon. Wea. Rev.* 2009; 137: 3471–3483. DOI: 10.1175/2009MWR2896.1
- [4] Edwards, R. Tropical cyclone tornadoes: A review of knowledge in research and prediction. *Electronic J. Severe Storms Meteor.* 2012; 7(6): 1–28.
- [5] Pearson, A D, Sadowski A F. Hurricane-induced tornadoes and their distribution. *Mon. Wea. Rev.* 1965; 93: 461–464. DOI: 10.1175/1520-0493(1965)093<0461%3AHITATD>2.3.CO%3B2
- [6] Smith, J S. The Hurricane-Tornado. *Mon. Wea. Rev.* 1965; 93: 453–457. DOI: 10.1175/1520-0493(1965)093<0453:THT>2.3.CO;2
- [7] Novlan, D J, Gray W M. Hurricane-Spawmed Tornadoes. *Mon. Wea. Rev.* 1974; 102: 476–488. DOI: 10.1175/1520-0493%281974%29102<0476%3AHST>2.0.CO%3B2
- [8] Gentry, R C. Genesis of Tornadoes Associated with Hurricanes. *Mon. Wea. Rev.* 1983; 111: 1794–1797:1802. DOI: 10.1175/1520-0493%281983%29111<1793%3AGOTAWH>2.0.CO%3B2
- [9] Baker, A K, Parker M D. Environmental Ingredients for Supercells and Tornadoes within Hurricane Ivan. *Wea. Forecasting.* 2008; 24: 225–226:242. DOI: 10.1175/2008WAF2222146.1
- [10] McCaul Jr., E W, Weisman M L. Simulations of Shallow Supercell Storms in Landfalling Hurricane Environments. *Mon. Wea. Rev.* 1995; 124: 426–427. DOI: 10.1175/1520-0493%281996%29124<0408%3ASOSSSI>2.0.CO%3B2
- [11] Spratt, S M, Sharp D W, Welsh P, Sandrik A, Alsheimer F, Paxton C. A WSR-88D Assessment of Tropical Cyclone Outer Rainband Tornadoes. *Wea. Forecasting.* 1997; 12: 498–499. DOI: 10.1175/1520-0434%281997%29012<0479%3AAWAOTC >2.0.CO%3B2
- [12] McCaul Jr., E W, Buechler D E, Goodman S J, Cammarata M. Doppler Radar and Lightning Network Observations of a Severe Outbreak of Tropical Cyclone Tornadoes. *Mon. Wea. Rev.* 2003; 132: 1758–1761. DOI: 10.1175/1520-0493%282004%29132<1747%3A DRALNO>2.0.CO%3B2

- [13] Edwards, R, Smith B T, Thompson R L, Dean A R. Analyses of Radar Rotational Velocities and Environmental Parameters for Tornadic Supercells in Tropical Cyclones. In: Proceedings of the 37th Conference of Radar Meteorology; 2006. p. 2:5-10.
- [14] Edwards, R. Tropical cyclone tornado records for the modernized National Weather Service era. In: Proceedings of the 25th Conference on Severe Local Storms; Denver, CO; 2010.
- [15] McCarthy, D, Schaefer J. Tornado trends over the past thirty years. In: Proceedings of the 14th Conference on Applied Meteorology, Seattle, WA; 2004.
- [16] Edwards, R, Dean A R, Thompson R L, Smith B T. Convective Modes for Significant Severe Thunderstorms in the Contiguous United States. Part III: Tropical Cyclone Tornadoes. *Wea. Forecasting.* 2012; 27: 1509–1510:1513-1518. DOI: 10.1175/WAF-D-11-00117.1
- [17] McCaul Jr., E W. Buoyancy and Shear Characteristics of Hurricane-Tornado Environments. *Mon. Wea. Rev.* 1991; 119: 1960:1965:1974-1977. DOI: 10.1175/1520-0493%281991%29119<1954%3ABASCOH>2.0.CO%3B2
- [18] Rasmussen, E N, Blanchard D O. A Baseline Climatology of Sounding-Derived Supercell and Tornado Forecast Parameters. *Wea. Forecasting.* 1998; 13: 1154:1158. DOI: 10.1175/1520-0434(1998)013<1148:ABCOSD>2.0.CO;2
- [19] Eastin, M D, Link M C. Miniature Supercells in an Offshore Outer Rain Band of Hurricane Ivan (2004). *Mon. Wea. Rev.* 2009; 137: 2102. DOI: 10.1175/2009 MWR2753.1
- [20] Thompson, R L, Mead C M, Edwards R. Effective Bulk Shear in Supercell Thunderstorm Environments. In: Proceedings of the 22nd Conference on Severe Local Storm; 2014.

IntechOpen

